Received: 21 March 2020 | Revised: 11 July 2020 | Accepted: 27 July 2020

DOI: 10.1002/bit.27521

ARTICLE

BIOTECHNOLOGY BIOENGINEERING WILEY

Dissolved oxygen concentration regulates human hepatic organoid formation from pluripotent stem cells in a fully controlled bioreactor

Zahra Farzaneh[1] | Saeed Abbasalizadeh[1,2] | Mohammad-Hassan Asghari-Vostikolaee[1] | Mehdi Alikhani[1] | Joaquim M. S. Cabral[2] | Hossein Baharvand[1,3]

[1]Department of Stem Cells and Developmental Biology, Cell Science Research Center, Royan Institute for Stem Cell Biology and Technology, ACECR, Tehran, Iran

[2]Department of Bioengineering and IBB - Institute for Bioengineering and Biosciences, Institute Superior Técnico, Universidade de Lisboa, Lisboa, Portugal

[3]Department of Developmental Biology, University of Science and Culture, Tehran, Iran

Correspondence
Hossein Baharvand, Department of Stem Cells and Developmental Biology, Cell Science Research Center, Royan Institute for Stem Cell Biology and Technology, ACECR, Banihashem Sq., Banihashem Street, Resalat Highway, P.O. Box 16635-148, Tehran 1665659911, Iran.
Email: Baharvand@Royaninstitute.org

Funding information
Iranian Council of Stem Cell Research and Technology; Iran National Science Foundation; Royan Institute; Ministry of Health and Medical Education, Grant/Award Number: 56700/147

Abstract

Developing technologies for scalable production of human organoids has gained increased attention for "organoid medicine" and drug discovery. We developed a scalable and integrated differentiation process for generation of hepatic organoid from human pluripotent stem cells (hPSCs) in a fully controlled stirred tank bioreactor with 150 ml working volume by application of physiological oxygen concentrations in different liver tissue zones. We found that the 20–40% dissolved oxygen concentration [DO] (corresponded to 30–60 mmHg pO_2 within the liver tissue) significantly influences the process outcome via regulating the differentiation fate of hPSC aggregates by enhancing mesoderm induction. Regulation of the [DO] at 30% DO resulted in efficient generation of human fetal-like hepatic organoids that had a uniform size distribution and were comprised of red blood cells and functional hepatocytes, which exhibited improved liver-specific marker gene expressions, key liver metabolic functions, and, more important, higher inducible cytochrome P450 activity compared to the other trials. These hepatic organoids were successfully engrafted in an acute liver injury mouse model and produced albumin after implantation. These results demonstrated the significant impact of the dissolved oxygen concentration on hPSC hepatic differentiation fate and differentiation efficacy that should be considered ascritical translational aspect of established scalable liver organoid generation protocols for potential clinical and drug discovery applications.

KEYWORDS

dissolved oxygen, fetal hepatic organoids, human pluripotent stem cells, red blood cells, stirred tank bioreactor

1 | INTRODUCTION

Liver diseases, including chronic and acute liver failure, are the fifth leading causes of mortality worldwide with over one million deaths annually (Alwahsh, Rashidi, & Hay, 2018; Olson, 2016). Although liver transplantation is a highly successful treatment for chronic liver diseases, it is the only available option. Increasing numbers of patients die each day or experience deteriorating health when placed on liver transplantation lists because of the critical local and worldwide shortages of available transplantable

livers. There are approximately 25,000 liver transplants are available worldwide per year (Dutkowski, Linecker, DeOliveira, Mullhaupt, & Clavien, 2015; Shukla, Vadeyar, Rela, & Shah, 2013). To cope with this unmet medical need, different research groups and companies have focused on developing promising regenerative medicine technologies that use different cell types as starting materials (e.g., human pluripotent stem cells [hPSCs], adult derived progenitors, and induced hepatocyte-like [iHep] cells from somatic cells) to generate functional hepatocyte-like cells, liver organoids, or tissue constructs (Yamamoto, Udono, Miura, Sekiya, & Suzuki, 2018) as therapeutic components for transplantation. These therapeutic components can be used to induce or assist the liver's inherent regeneration capacity and hopefully treat acute or chronic liver failure (Zhang et al., 2018). Among the different available cell sources, hPSCs are considered one of the most convenient cell types. These cells provide an unlimited source for integrated hepatic differentiation and scalable production of hepatocyte-like cells or liver organoids for translational studies and clinical applications, and are easily amenable for scalable expansion and integrated differentiation (Abbasalizadeh, Larijani, Samadian, & Baharvand, 2012; Kwok et al., 2018). However, most studies have used small and/or static (culture dishes and multi-well plates) or dynamic culture (spinner flasks) systems with limited culture working volumes (1.5–50 ml) and uncontrolled culture conditions in an attempt to establish protocols to generate hepatocyte-like cells or hepatic organoids from hPSCs (Pettinato et al., 2019; Sgodda et al., 2017; Takebe et al., 2013, 2017). These culture systems are convenient for protocol development and optimization studies; however, they lack adequate scalability to produce clinically relevant cell numbers ($1–2 \times 10^9$ cells/patient) as essential therapeutic components to treat one or multiple patients with autologous or allogeneic cell therapy strategies (Tzanakakis, Hess, Sielaff, & Hu, 2000). Therefore, this critical technical issue has largely hindered the potential use of currently established protocols for clinical or commercial applications (Sgodda et al., 2017; Vosough et al., 2013). Other critical issues that should be addressed in established protocols of small scale cultures include issues with quality of the final product such as low differentiation efficacy and functionality of hepatocytes (e.g., poor gene expression profiles and metabolic characteristics) compared to primary hepatocytes; productivity issues such as low cell yields; product homogeneity; and lack of process reproducibility that could be potentially boosted during scale-up trials (Vosough et al., 2013). Thus, development of robust bioprocess technologies for scalable production of human functional hepatocytes or hepatic organoids is a necessary step before the clinical translation of currently developed regenerative medicine technologies.

Previously, we improved the efficacy of our protocol for stepwise and integrated hepatic differentiation of hPSCs as three-dimensional (3D) aggregates in a 50 ml dynamic suspension culture by optimizing a hepatic endoderm differentiation strategy (e.g., CHIR and activin A concentration and treatment time) and explored the optimal hPSCs starting aggregate size for beginning the differentiation process (Farzaneh, Najarasl, Abbasalizadeh, Vosough, & Baharvand, 2018). However, we realized that our protocol was not scalable after a ×3 volume increase to a 150 ml working volume under the same uncontrolled dynamic culture condition and resulted in the generation of heterogeneous hepatospheres that had limited functionality. Next, we employed fully controlled culture conditions in a bioreactor to scale-up our established integrated hepatic differentiation protocol by regulating pH and optimizing dissolved oxygen (DO) concentrations in the range of liver tissue physiological oxygen concentrations, as a very important cue in hepatic fate determination and liver function (Kietzmann, 2017). To date, the results of different studies have demonstrated the significant effect of oxygen concentration/gradient on hPSCs hepatic differentiation efficacy, functionality, and maturation. Blood oxygen concentration modulates liver zonation and metabolic activity (Jungermann & Kietzmann, 2000; Khakpour et al., 2017; Nishikawa et al., 1996; Pimton et al., 2015) as well as hepatic differentiation from human hPSCs by regulation through intercellular transforming growth factor β (TGFB) signaling (Ayabe et al., 2018). However, generation of hepatocyte-like cells or liver organoids in fully controlled stirred bioreactors and exploring the effect of DO concentration on integrated hepatic differentiation efficacy of hPSCs as 3D aggregates has not been studied. Therefore, we used a stirred tank bioreactor to develop a fully controlled integrated hepatic differentiation process and explored the effect of different oxygen concentrations (20%, 30%, and 40% air saturation, which corresponded to 30–60 mmHg pO_2 within liver tissue) on process efficacy and quality attributes of the final product. Stirred suspension/tank bioreactors have been successfully used for scalable production of hPSCs and their potential therapeutic derivatives such as beating cardiomyocytes (Fonoudi et al., 2015), neural stem cells (Nemati, Abbasalizadeh, & Baharvand, 2016), and hepatocytes (Vosough et al., 2013), and can be considered a superior option for large-scale production of hPSC derivatives, including hepatocyte-like cells and hepatic organoids.

Here, the application of an optimized DO concentration (30% air saturation at 37°C, equal to 40–45 mmHg pO_2 in liver tissue) resulted in the generation of self-organized fetal-like hepatic organoids comprised of functional hepatocytes and red blood cells. We observed that employing 20% DO and uncontrolled culture condition resulted in generation of hepatospheres that had poor functionality and homogeneity. The demonstrated cross-talk between hepatocytes and erythroid cells, which also occurs during human liver bud development, resulted in improved metabolic activity, functionality, and meaningfully higher levels of CYP enzyme activity of the hPSC-derived fetal-like hepatic organoids generated in our study (Dzierzak & Speck, 2008). Our data emphasized and highlighted the critical effect of oxygen concentration on integrated differentiation efficacy of hPSCs and its fate determination properties as 3D aggregates, which should be explored and optimized before clinical translation and the commercialization stage of established protocols.

2 | MATERIALS AND METHODS

The Supporting Information provides detailed materials and methods for molecular and biochemical characterization of the cells and organoids, functional studies, and the mice transplantation study.

2.1 | Expansion and integrated hepatic differentiation of hPSCs under a dynamic suspension culture condition

RH5 cells were cultured as previously described as 3D aggregates under a dynamic suspension culture in a 250 ml glass stirred bioreactor vessel with a 150 ml working volume that used human foreskin fibroblast conditioned hPSC medium (Farzaneh et al., 2018). Briefly, the agitation rate was set to 40 rpm during the hPSCs expansion and integrated differentiation process. The integrated hepatic differentiation process for hPSC aggregates under the dynamic suspension culture was conducted in three developmental steps. In the endoderm differentiation step, we used a basal medium that included RPMI 1640 plus B-27 supplement without vitamin A (×1) and CHIR99021 (CHIR, 6 μM). After 24 hr, we added basal medium supplemented with activin (10 ng/ml) for 48 hr. For the hepatic differentiation step, Dulbecco's modified Eagle's medium/F12 plus KOSR (2% vol/vol) supplemented with hepatocyte growth factor (HGF, 10 ng/ml) and fibroblast growth factor (FGF4, 10 ng/ml) was used for 6 days. Afterwards, 50% (vol/vol) of the previous medium was replaced by hepatocyte culture medium that contained oncostatin M (OSM, 10 ng/ml) and dexamethasone (10^{-7} M) for 11 days.

2.2 | Integrated hepatic differentiation of hPSCs under fully controlled culture conditions in a stirred tank bioreactor

We conducted all the bioreactor runs in an in-house made 250 ml glass stirred bioreactor vessel with maximum 150 ml working volume, which was equipped with a glass bulb impeller placed on a magnetic stirrer platform in a 37°C temperature-controlled chamber. The vessel was equipped with pH and DO probes, and fully monitored and controlled by a PC-based stirred tank bioreactor (New Brunswick™ CelliGen 310 and BioCommand software). Both integrated and fully controlled hepatic differentiation processes in the bioreactor and its uncontrolled culture condition counterpart (control group) had an equal working volume of 150 ml with a 40-rpm agitation rate. The DO concentrations (20%, 30%, and 40% air saturation) were monitored by a polarographic DO probe and automatically regulated by a cascading DO setpoint at three stepwise levels with Air, N_2, and O_2 sparging/flow rates using the bioreactor four-gas mixing system equipped with four solenoid valves/thermal mass flow controllers (TMFCs) to control each gas flow rate (0.08–2 VVM) under the control of the bioreactor controller software. The pH was maintained at 7.2 ± 0.1 by cascading the pH module with the CO_2 gas flow rate regulated by TMFC. All gasses were passed through a 0.2 μm membrane and humidifier, and then sparged into the head space of the culture vessel when needed by the gas mixing system.

2.3 | Statistical analysis

We used a dedicated uncontrolled bioreactor culture for each of the DO concentration trials with the same cell source and differentiation protocol. We included three biological replicates for each of the different DO concentrations. These samples were derived from 1.5 to 2 ml of suspension collected from different time points of the bioreactor runs. Data are presented as mean ± standard deviation (*SD*). Comparisons between groups and data were performed with one-way analysis of variance and the post hoc Tukey's test. $p \leq .05$ was considered to be statistically significant.

3 | RESULTS

3.1 | Online monitoring of DO concentration and pH during integrated hepatic differentiation of hPSC aggregates in the stirred bioreactor

The hPSC 3D spheroids (~150 μm mean aggregate diameter; hereafter named hPSpheres, Figure S1A) were differentiated into a hepatic lineage in three developmental steps that included generation of endodermal cells (endospheres), hepatoblasts (hepatoblastspheres), and hepatocyte-like cells (hepatospheres) over a 20-day culture period as previously described (Figure 1a; Farzaneh et al., 2018). We used a fully controlled stirred tank bioreactor with a 150 ml working volume to scale-up our established protocol in a 50 ml working volume. Key bioprocesses parameters were monitored during the integrated differentiation to identify potentially important parameters that possibly influenced hepatic differentiation efficacy and might result in the generation of heterogeneous hepatospheres with low functionality and metabolic activity (Figure 1b). Online monitoring of the hepatic differentiation process in the 150 ml working volume under uncontrolled culture conditions revealed unstable and decreasing DO and pH profiles during the different stages of differentiation. The oxygen concentration was not limited during endoderm differentiation (Day 3) and hepatoblast generation (Day 9 of the integrated differentiation process). However, the oxygen concentration dramatically decreased during the hepatocyte expansion and maturation phase, from approximately 70% after medium refreshment to 5–20% air saturation during 10–20 days of culture. Hence, we considered the oxygen concentration as a variable and a potentially limiting factor during the integrated hepatic differentiation process that should be optimized accordingly (Figure 1c). We observed that the pH level was unstable and decreased from 7.8 to 6.2 after medium refreshment, even with continuous introduction of air with 5% CO_2 into the vessel headspace for pH control, which is a

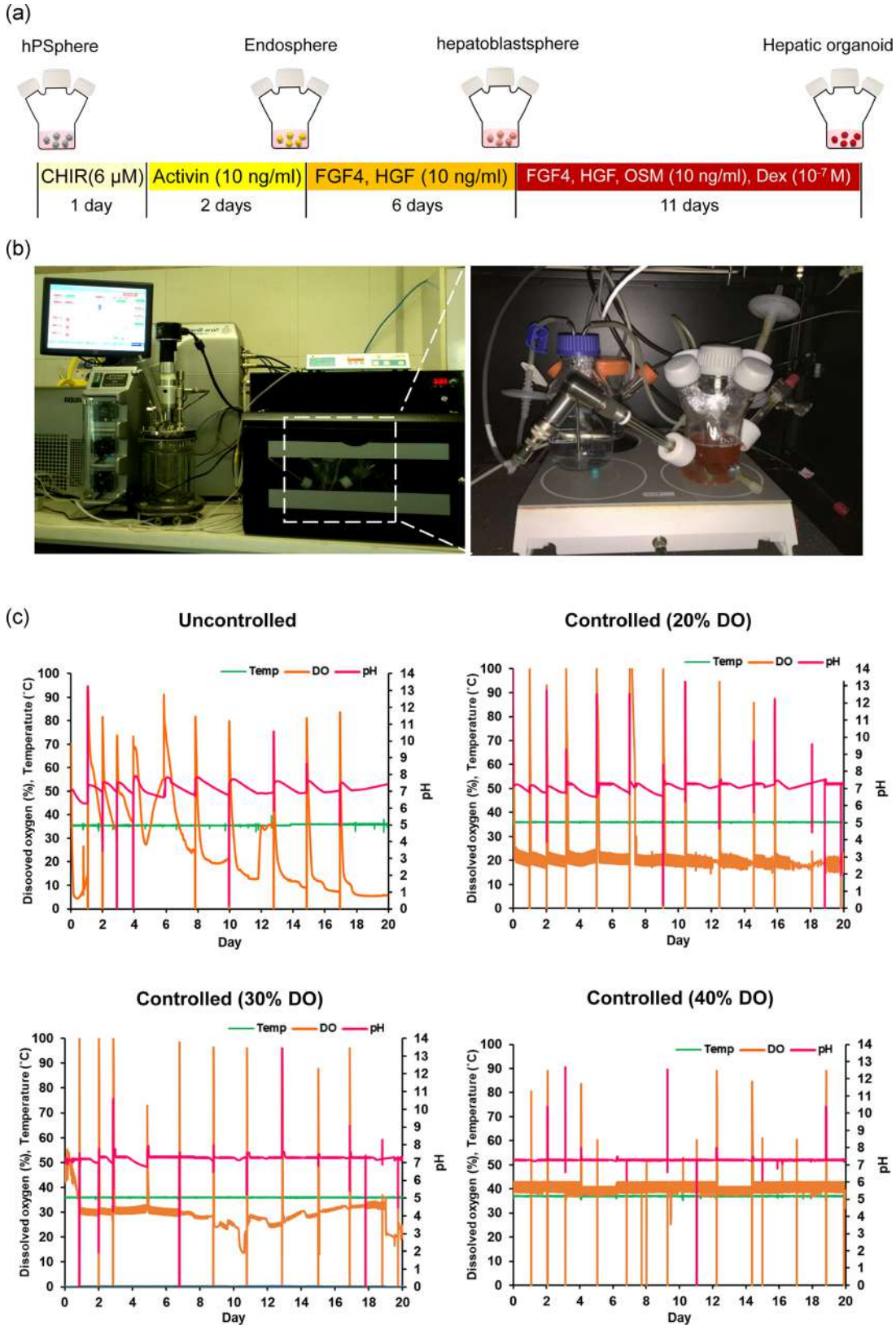

FIGURE 1 Integrated hepatic differentiation of hPSC 3D spheroids (hPSpheres) into hepatic organoids in a stirred tank bioreactor under fully controlled conditions. (a) Schematic diagram of hepatic organoid generation from hPSpheres. (b,c) A stirred tank bioreactor with a 150 ml working volume under uncontrolled or fully controlled conditions of 20%, 30%, and 40% DO at pH 7.2, and online monitoring trend lines of temperature, DO, and pH for different trials. 3D, three dimensional; DO, dissolved oxygen; hPSC, human pluripotent stem cell [Color figure can be viewed at wileyonlinelibrary.com]

standard strategy for maintaining a constant pH during the culture condition. Therefore, we developed a strategy to control the DO concentration (20%, 30%, and 40% air saturation, equal to 30, 45, and 60 mmHg, respectively, at 37°C) in similar range of pO_2 in different regions of the human liver tissue (Brooks, Hammond, Girling, & Beckingham, 2007) and regulated the pH precisely at 7.2 ± 0.1 during different steps of the hepatic differentiation process in an attempt to improve efficacy and productivity of the hepatospheres. The results of all bioreactor runs were compared to their uncontrolled culture condition counterpart, which was conducted under the same time and operation conditions of cell source, working volume, culture vessel, differentiation protocol, and operation time.

3.2 | The effect of regulating DO concentration on integrated differentiation efficacy into endodermal cells and hepatoblasts

In the first step, we evaluated the endosphere differentiation efficacy of hPSpheres at different DO concentrations after 3 days of the stepwise

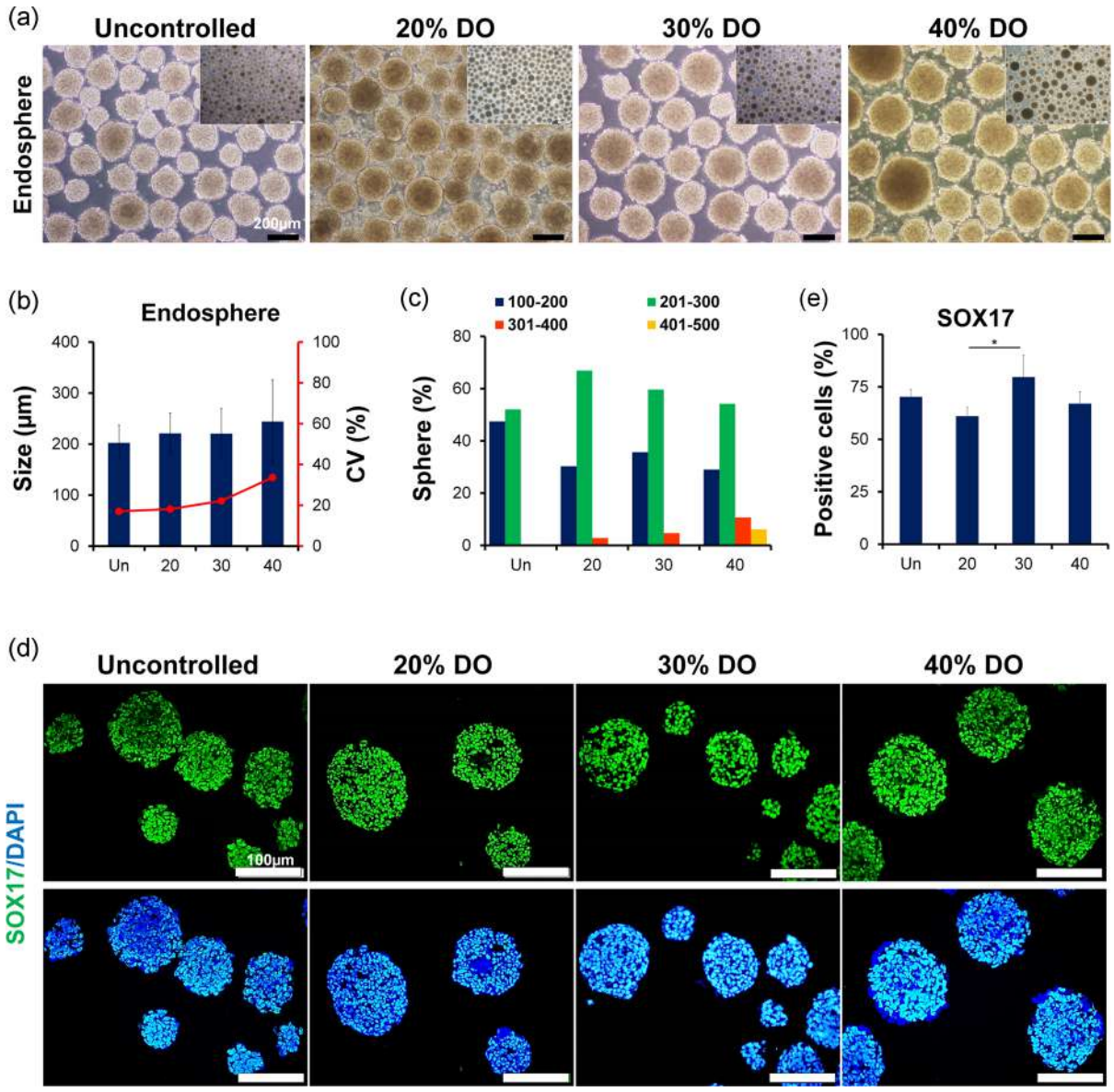

FIGURE 2 The effect of controlled DO on differentiation to endodermal cells. (a) The morphology of endospheres was relatively similar between groups. Scale bar = 200 μm. Mean size with CV (b) and (c) size distribution of endospheres. Histogram data showed that size heterogeneity increased under 40% DO conditions. About 150–200 spheres were counted in each experimental group. (d) Immunofluorescent images of sectioned endospheres under different culture conditions. (e) Flow cytometry data showed a similar percent of SOX17-positive cells among the groups. The percentage of SOX17 positive cells was higher under 30% DO than 20% DO. Scale bar = 100 μm. Data (mean ± *SD*) were analyzed with ANOVA and Tukey's post hoc test; $n = 3$. 20%, 30% and 40%, differentiation under DO controlled culture conditions in a stirred bioreactor with 20%, 30%, and 40% DO. ANOVA, analysis of variance; CV, coefficient of variation; DAPI, 4′,6-diamidino-2-phenylindole; DO, dissolved oxygen; Un, differentiation under uncontrolled culture condition. $^*p < .05$ [Color figure can be viewed at wileyonlinelibrary.com]

and integrated differentiation process. The generated endospheres had a relatively similar morphology under both the controlled and uncontrolled conditions (Figure 2a). We measured the aggregate diameters to estimate cell proliferation kinetics during each point of the stepwise hepatic differentiation. The endospheres had a round and dense morphology with a 220 µm mean diameter size under all culture conditions, except for 40% DO (Figure 2b). The 40% DO resulted in larger endospheres (244 ± 82 µm) with an approximately 33% coefficient of variation (CV), which showed increased heterogeneity of the endosphere sizes (Figure 2b,c). Immunostaining results indicated that the SOX17-positive cells were distributed and well-expressed in each single endosphere under different culture conditions (Figure 2d). Flow cytometry analysis also showed that approximately 70% of the cell populations expressed SOX17 under uncontrolled, 20% DO, and 40% DO conditions. The highest SOX17 expression was under 30% DO (about 80%) and was significantly higher than 20% DO ($p \leq .05$; Figures 2e and S2). Thus, controlling the DO concentration during endoderm differentiation resulted in higher expressions of endoderm markers at 30% DO and lower expressions at 20% DO. In the next step, the endospheres were treated for an additional 6 days in HGF and FGF4 supplemented medium for integrated differentiation to hepatoblasts as 3D aggregates (hepatoblastspheres). The hepatoblastspheres generated in all of the trials had a round and mostly dense morphology (Figure 3a,f, 4′,6-diamidino-2-phenylindole staining). The aggregate mean diameter size increased in the higher DO concentrations until it reached a maximum diameter of 260 µm at 40% DO with higher CV compared with the other groups (Figure 3b). The hepatoblastsphere size distribution was more homogenous at 20% and 30% DO, and increased heterogeneity was observed under the uncontrolled and 40% DO conditions (Figure 3b,c). Gene expression analysis showed that the hepatoblasts generated in all groups well-expressed *α-fetoprotein* (*AFP*), albumin *(ALB)*, *HNF4A*, and *TTR* in a similar manner (Figure 3d). AFP expression, as a key marker of hepatic progenitors, was also validated by western blot analysis. The results showed no significant differences in AFP expression levels among the different trials (Figures 3e and S3A). Immunostaining analysis also showed that AFP was well-expressed in the cytoplasm of cells distributed through all hepatoblastspheres generated under the different trials, except for those generated under 20% DO where AFP expression was not detected in some spheres. E-cadherin (E-cad), an early surface hepatic marker, expressed in cells that were mainly located around the hepatoblastspheres under fully controlled DO conditions, which was similar to liver organoids derived from the human liver (Figure 3f). Thus, the results of gene and protein expression analyses indicated that the integrated differentiation efficacy to hepatoblasts was similar under the controlled DO conditions and the uncontrolled condition.

3.3 | Generation of human fetal-like hepatic organoids during integrated hepatoblast expansion and maturation

There was a significant change in hepatosphere morphology after Day 11 in both the fully controlled and uncontrolled conditions (Figure 4a). The average diameter sizes of Day 20 hepatospheres in all groups were approximately 370 µm, except for the 30% DO group that had a smaller diameter size compared to the other conditions (mean diameter: approximately 300 µm) with more uniform morphology and lower CV (Figure 4b,c). More important, the fully controlled conditions significantly decreased the generation of hepatospheres that had cystic morphologies. The majority of hepatospheres generated under the uncontrolled culture condition had a cystic/transparent (59 ± 9%) structure and morphology (Figure 4d) compared to 4 ± 0.1% at 20% DO ($p < .001$), 16 ± 10% at 30% DO ($p < .01$), and 30 ± 12% at 40% DO. These results indicated that the fully controlled culture condition could reduce final product morphology heterogeneity in favor of dense hepatosphere production (Figure 4a,d). Third, measurement of total DNA content in the final products, as an indirect method for estimation of cell numbers, showed that the total cell production yield after the 20-day culture increased by 1.4–1.6-fold under the fully controlled conditions compared to the uncontrolled culture conditions ($p < .01$; Figure 4e).

Fourth, we observed the appearance of red cell clusters inside the hepatic endoderm aggregates under 30% DO and 40% DO controlled conditions, which was an interesting morphological change.

The red spots in the aggregates were visible from 11 to 13 days of the integrated hepatic differentiation and these areas were increasing onward until Day 20. We counted the hepatospheres with red spots at Day 20 and found that 27.8 ± 6.3% and 31.7 ± 6.0% of the total hepatospheres (small or large, cystic or dense) contained red blood cells under 30% and 40% DO, respectively (Figure 4f). The red cells generated within the hepatospheres were characterized after harvesting all aggregates at the end of the differentiation process (Figure 4g,h).

Flow cytometry analysis of these red cell populations revealed a relatively small population of cells that expressed early erythroblast markers CD36 and CD71. Approximately 13 ± 2% of this population expressed CD36 in 30% DO and 14.5 ± 5% in 40% DO, whereas 16 ± 4% of cells expressed CD71 in 30% DO and 25.5 ± 7% in 40% DO (Figure 4g). CD235a, an erythroid precursor surface marker, was expressed in 18 ± 12% of the hepatosphere cell population under 30% DO and in 29.5 ± 3.5% of these cells under 40% DO. A significant difference existed in expressions of these markers under 30% DO and 40% DO compared to the uncontrolled culture condition, where approximately 4 ± 5% of the erythroid markers were expressed with the same differentiation culture media and strategy. This data showed a direct effect of increased DO concentration on regulation of the hPSC fate inside the hepatic endoderm aggregates, which resulted in co-generation of hepatocytes and red blood cells.

We evaluated relative RNA expression of *α-*, *γ-*, and *β-globin*, an erythroid specific marker, in hepatospheres generated under controlled and uncontrolled conditions, and compared the results to nucleated red blood cells (nRBC) derived from cord blood (positive control; Figure 4h). Cell populations derived from 30% DO ($p < .001$) and 40% DO ($p < .05$) expressed fetal erythroid markers such as *α-* and *γ-globin* at significantly higher levels than the uncontrolled

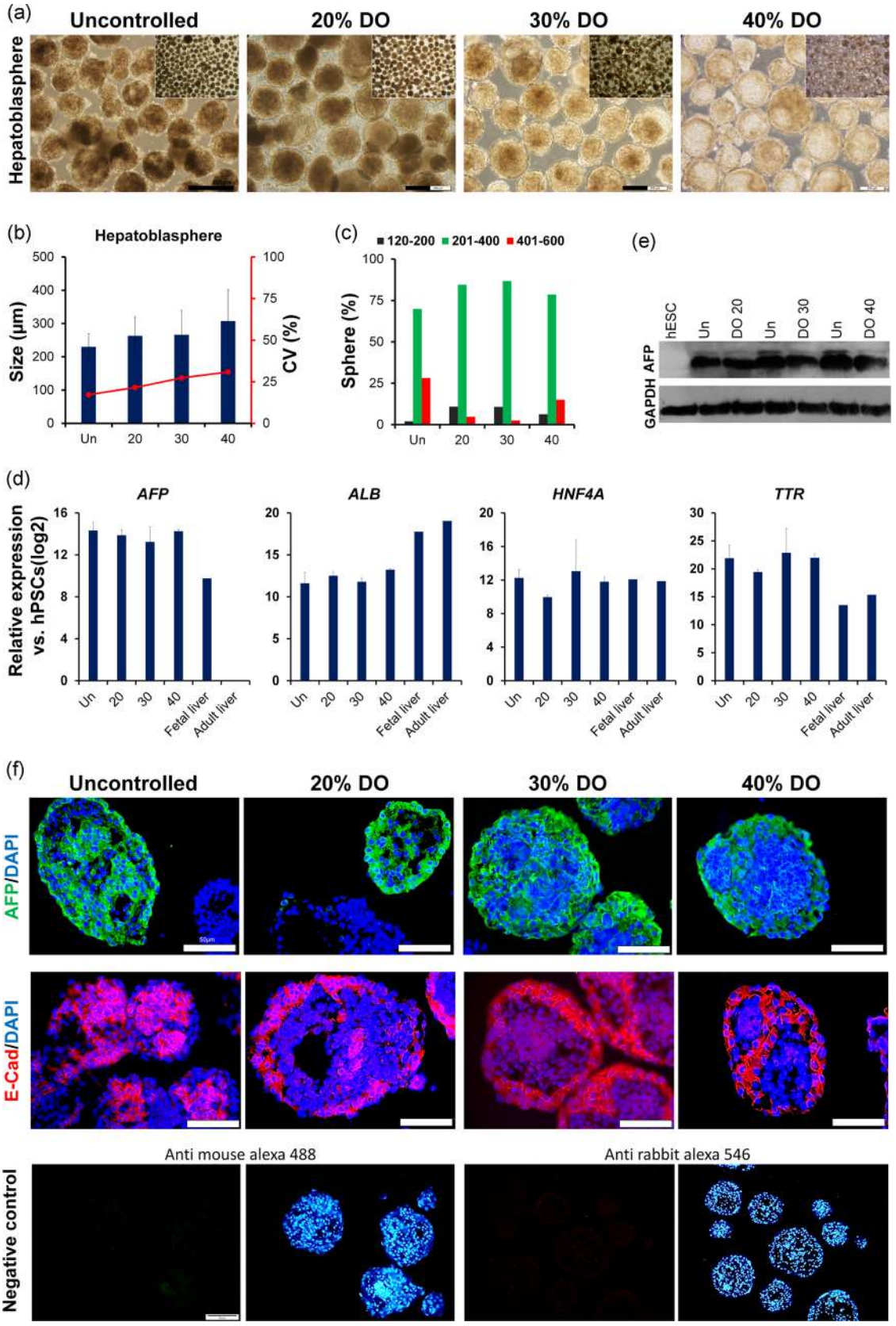
(a)
Uncontrolled
20% DO
30% DO
40% DO
Hepatoblasphere
(b)
Hepatoblasphere
Size (μm)
CV (%)
Un
20
30
40
(c)
120-200
201-400
401-600
Sphere (%)
(e)
hESC
Un
DO 20
DO 30
DO 40
GAPDH
AFP
(d)
AFP
ALB
HNF4A
TTR
Relative expression vs. hPSCs(log2)
Fetal liver
Adult liver
(f)
AFP/DAPI
E-Cad/DAPI
Negative control
Anti mouse alexa 488
Anti rabbit alexa 546

condition. *β-globin*, an adult *HB*, was expressed at low levels in these cell populations. *HB* expression in the hepatic organoids was lower than in nRBC, which demonstrated the fetal nature of these generated erythroid cells within the hepatospheres.

Quantitative reverse-transcription polymerase chain reaction (qRT-PCR) analysis was performed on Days 3, 9, and 20 to assess the temporal expressions of the mesoderm and hematopoeitic markers at 30% and 40% DO.

MIXL1, a hematopoiesis promoter and mesoendodermal marker (Ng et al., 2005), upregulated significantly at Day 3 of differentiation under the fully controlled culture condition (Figure 4i). However, the expressions of the mesodermal and hematopoiesis markers, *T* or *Brachyury* and *KDR* (Goldman, Cohen, & Gouon-Evans, 2016; Han, Goldman, & Gouon-Evans, 2014; Ziegler et al., 1999) did not change significantly at Day 3. Day 9 gene expression results showed that *RUNX1*, *HOXA9*, *HOXB4*, *DLL4*, and *PECAM* were significantly upregulated under controlled conditions compared to the uncontrolled condition. *RUNIX1* is a master regulator of hematopoiesis, which is essential in the initial and final stages of hematopoiesis (Yzaguirre, de Bruijn, & Speck, 2017). *HOXA9* (Ramos-Mejia et al., 2014) and *HOXB4* are important for hematopoietic stem cell (HSC) fate determination (Forrester & Jackson, 2012). *DLL4* and *PECAM* are important for both HSC maintenance (Ayllon et al., 2015) and erythroid lineage commitment (Baumann et al., 2004).

Expression analysis of the cells at Day 20 showed a significant increase in *LMO-2* expression (HSC and erythropoiesis marker; Brandt & Koury, 2009) under controlled conditions compared to the uncontrolled culture condition (Figure 4i). There were no significant changes in expressions of *PU.1* (marker for myeloid or lymphoid precursors cells; Burda, Laslo, & Stopka, 2010), *SOX4* (lymphoid marker; Laurenti et al., 2013), *GATA2* (HSC and erythroid lineage; Vicente, Conchillo, Garcia-Sanchez, & Odero, 2012), and also hepatoblast markers (Goldman et al., 2016; Figure 4i). These results indicated that the DO concentration regulated the fate of the hPSC aggregates through endoderm as well as mesoderm induction. This regulation was concentration-dependent. Regulation of DO at higher (30%) air saturation resulted in partial generation of mesoderm cells, an erythroid lineage, and subsequently red blood cells in addition to endodermal, hepatic endoderm, and hepatic cells.

We quantified the hepato-specific gene expressions of the differentiated cells after 20 days of integrated differentiation and found that hepatocyte cells were generated under all of the tested conditions and they expressed the basic hepatic markers *TTR*, *AFP* and *ALB*. The expression levels of these basic hepatic markers were comparable to fetal liver expression levels; however, they were not similar to the adult liver expression pattern because *AFP* is not normally expressed in the adult liver (Figure 5a). Gene expression analysis results showed that fully controlled integrated differentiation at 30% DO resulted in the highest expression of important mature hepatic markers *(CYP3A*, *G6PC)* compared to the other DO concentrations and the uncontrolled culture condition, which provided evidence for the enhanced maturation and functionality of these generated cells ($p < .001$). In contrast to 30% DO, expressions of other hepatic markers *(CYP3A7*, *CYP3A4*, *PEPCK*, *G6PC*, *TAT*, and *TDO)* significantly downregulated in 20% DO and *TAT* significantly downregulated in 40% DO compared to the uncontrolled culture condition (Figure 5a). We also evaluated hepatic nuclear factor expressions in the differentiated cells. *HNF4A* and *HNF1B* had significantly lower expressions in the 20% and 40% DO conditions compared to the uncontrolled condition, as well as *HNF6A* expression at 30% and 40% DO compared to the uncontrolled and 20% DO conditions (Figure 5a).

We attempted to conduct a cell population study of the generated hepatospheres with different treatments. However, we were unable to dissociate the hepatospheres into viable single cell populations for flow cytometry analysis when we used different enzymatic or mechanical treatments or their combinations because of the highly intact structure of these hepatospheres. We hypothesized that the hepatospheres became intact in response to dynamic shear stress in the stirred bioreactor by the secretion of the ECM around the spheres. To obtain a rough estimate of the number of ALB-positive cells in the hepatic organoids, we counted the ALB-positive cells in different immunofluorescent images of the cross-sectioned hepatospheres. The results showed that about 35% of the population per microscopic field were ALB-positive under the 30% DO condition (Figures 5b and S1B) and were dispersed in all hepatosphere sizes and morphologies (Figure S1B). The ALB-positive cells were significantly less under the 20% DO condition compared with the other groups ($p \leq .05$; Figures 5b and S1B).

Data from western blot analysis also confirmed the expressions of AFP and ALB in all of the trials (Figure 5c). Quantitative analysis showed significantly lower expressions of AFP ($p < .05$) and ALB ($p < .01$) in the 20% DO group compared to the uncontrolled, 30% DO, and 40% DO groups. These markers had similar expression

FIGURE 3 The effect of controlled DO on hepatoblast differentiation. (a) Hepatoblastspheres in different groups had a similar morphology. Scale bar = 200 μm. (b) and (c) Mean size, CV, and size distribution of hepatoblastspheres. The mean size of the hepatoblastspheres was 260 μm; 70% of the hepatoblaspheres were 200–400 μm. About 100–150 spheres were counted in each experimental group. (d) Gene expression analysis of hepatoblastspheres showed high expression levels of *TTR*, *AFP*, *HNF4A*, and *ALB* in the groups. (e) Western blot for AFP expression in hepatoblastspheres. (f) Representative immunofluorescent images of sectioned hepatoblastspheres in different conditions showed expressions of AFP and E-cad. Scale bar = 50 μm. Data (mean ± *SD*) were analyzed with ANOVA and Tukey's post hoc test; $n = 3$. 20%, 30%, and 40%, differentiation under DO controlled culture conditions in the stirred bioreactor; AFP, α-fetoprotein; ALB, albumin; CV, coefficient of variation; DAPI, 4′,6-diamidino-2-phenylindole; DO, dissolved oxygen; E-cad, E-cadherin; Un, differentiation under uncontrolled culture condition [Color figure can be viewed at wileyonlinelibrary.com]

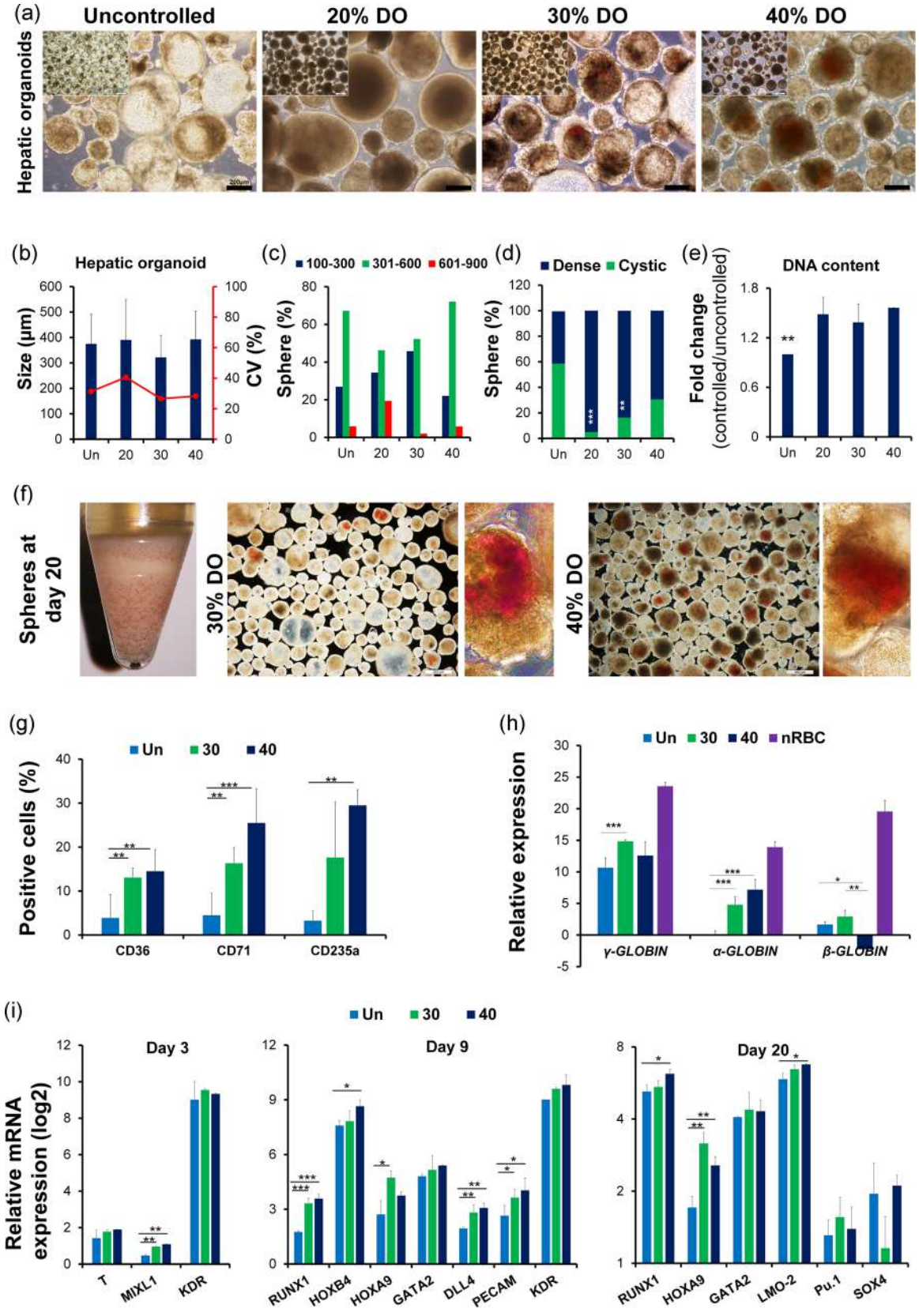
(a)
Uncontrolled
20% DO
30% DO
40% DO
Hepatic organoids
(b)
Hepatic organoid
Size (μm)
CV (%)
Un 20 30 40
(c)
100-300 301-600 601-900
Sphere (%)
(d)
Dense Cystic
Sphere (%)
(e)
DNA content
Fold change (controlled/uncontrolled)
(f)
Spheres at day 20
30% DO
40% DO
(g)
Un 30 40
Positive cells (%)
CD36 CD71 CD235a
(h)
Un 30 40 nRBC
Relative expression
γ-GLOBIN α-GLOBIN β-GLOBIN
(i)
Un 30 40
Relative mRNA expression (log2)
Day 3
T MIXL1 KDR
Day 9
RUNX1 HOXB4 HOXA9 GATA2 DLL4 PECAM KDR
Day 20
RUNX1 HOXA9 GATA2 LMO-2 Pu.1 SOX4

patterns in the 30% DO and 40% DO groups (Figure S3B). To assess the morphology of hepatocytes generated within hepatospheres under the two-dimensional (2D) culture condition, we plated hepatospheres that had been generated under the 30% DO condition on Matrigel-coated plates. After 3 days of plating, polygonal cells with large nuclei had migrated from each hepatosphere (Figure 5d). We observed that they expressed AFP, ALB, CYP1A1, and ASGPR as demonstrated by immunostaining (Figure 5e).

These results demonstrated the co-generation of functional fetal hepatocyte-like cells and red blood cell populations within hepatospheres after 20 days of integrated differentiation under the 30% and 40% DO concentrations. Thus, we called these hepatospheres fetal-like hepatic organoids because of their similar cell population and functionality to the human fetal liver, which is mainly populated by these two cell types.

To further evaluate the functionality of the generated hepatocyte-like cells within these organoids, we analyzed the metabolic activity of these cells by exploring the secretion profiles of hepatic specific metabolites in samples collected from hepatic organoid conditioned medium after Day 20 of differentiation (Figure 6a–d). The hepatic organoids generated under 30% and 40% DO had relatively higher secretion levels of ALB (Figure 6a) and fibrinogen (Figure 6b) compared to the 20% and uncontrolled conditions. In addition, hepatospheres and hepatic organoids derived under all of the tested conditions had the ability to produce urea as a key and essential metabolic activity of hepatocytes (Figure 6c). The drug detoxification ability of hepatic organoids was also tested by analysis of CYP3A4 activity, as an important enzyme of xenobiotic metabolism. We treated the hepatic organoids with rifampicin, a CYP3A4 inducer, for 3 days and compared the results to the DMSO control group, which represented basal CYP3A4 enzyme activity in the hepatocytes. The results showed a significant fold increase in CYP3A4 enzyme activity compared to DMSO in the 30% DO condition and a decrease in the 20% DO (Figure 6d). Further evaluation of these cells in the 30% DO condition showed that they had additional hepatic specific functions of indocyanine green (ICG) and low-density lipoprotein (LDL) uptake, as well as glycogen storage in their cytoplasm in the uncontrolled culture condition (Figure 6e). Uptake results showed that about 59.0 ± 9.9% and 71.1 ± 13.5% of the hepatospheres could uptake ICG and became partially or entirely green under the uncontrolled and 30% DO conditions, respectively. Additionally, 76.5 ± 5.6% of the hepatospheres could uptake LDL under the uncontrolled culture condition and 78.4 ± 7.6% could uptake LDL under the 30% DO condition.

Altogether, differentiation under the 30% DO controlled bioreactor condition resulted in the generation of fetal-like hepatic aggregates that had a more homogenous morphology and diameter size distribution, higher cell yield, hepatic metabolic activity (particularly *CYP* activity), hepatic functions, and gene expression compared with the other DO concentrations and the uncontrolled culture condition.

Finally, to demonstrate the in vivo functionality of hepatic organoids generated under the fully controlled condition, we transplanted the whole organoids derived under the 30% DO condition into the spleen of an acute liver mouse model. We observed a human ALB-positive cell population that was distributed as clusters or single cells within the mice spleens at 7- and 14-day post-transplantation (Figure 6f). Most human ALB-positive cells were positioned around the large capillaries in the liver on days 7 and 14 post-transplantation (Figure 6f). These cells secreted 2.5 ± 1 ng/ml human ALB into the mice sera 7 days post-transplantation and 3.4 ± 0.7 ng/ml human ALB into the mice sera 14 days post-transplantation (Figure 6g). The results indicated that the human fetal-like hepatic organoids had successfully engrafted into the spleen and liver of the mouse model, and had a demonstrated ability to secrete human ALB into the mice sera.

3.4 | Reproducibility of the developed integrated hepatic differentiation process at the 30% DO concentration

Finally, we validated the reproducibility of the developed integrated differentiation process by conducting three independent bioreactor

FIGURE 4 The effect of controlled DO on differentiation to hepatocyte-like cells. (a) Morphology of hepatic organoids differed among the groups. Scale bar = 200 μm. (b,c) Mean size, CV, and size distribution of hepatic organoids. The mean size of the hepatic organoids was approximately 370 μm. The size distribution of the hepatic organoids showed a vastly distributed heterogeneous population, except under the 30% DO condition. About 70–150 spheres were counted in each experimental group. (d) Different appearance of hepatic organoids, dense or cystic. Hepatic organoids under the uncontrolled culture condition had a significantly more cystic population than the controlled condition. (e) Fold change of cells by total DNA concentration of hepatocytospheres. DNA concentration showed an increase in the total yield of cells produced under the controlled conditions. (f) Controlled bioreactor produced red clusters in hepatic organoids under 30% and 40% DO conditions. Morphology of red clusters inside the hepatic organoids. During differentiation of hepatoblasts to hepatocytes, we observed the appearance of a number of red clusters in spheres in the 30% or 40% DO conditions harvested after 20 days of culture. (g) Flow cytometry data for erythroid markers. Flow data revealed that a small fraction of the dispersed hepatic organoids expressed erythroid precursor markers CD36, CD71, and CD235a. (h) qRT-PCR data for *α*-, *γ*- and *β-globin* expressions showed that samples derived under 30% and 40% DO controlled conditions significantly expressed *α-globin* and *γ-globin*, but not *β-globin*, compared to the uncontrolled condition. Nucleated RBCs derived from cord blood were used as the positive control that highly expressed all *globin* genes. (i) qRT-PCR data for expression of HSC markers during three differentiation steps. Data (mean ± *SD*) were analyzed with ANOVA and Tukey's post hoc test. 20%, 30%, and 40%, differentiation under DO controlled culture conditions in stirred bioreactor; CV, coefficient of variation; DO, dissolved oxygen; nRBC, nucleated red blood cell; qRT-PCR, quantitative reverse-transcription polymerase chain reaction; Un, differentiation under uncontrolled culture condition. $n = 3$. $^{*}p < .05$; $^{**}p < .01$; $^{***}p < .001$ [Color figure can be viewed at wileyonlinelibrary.com]

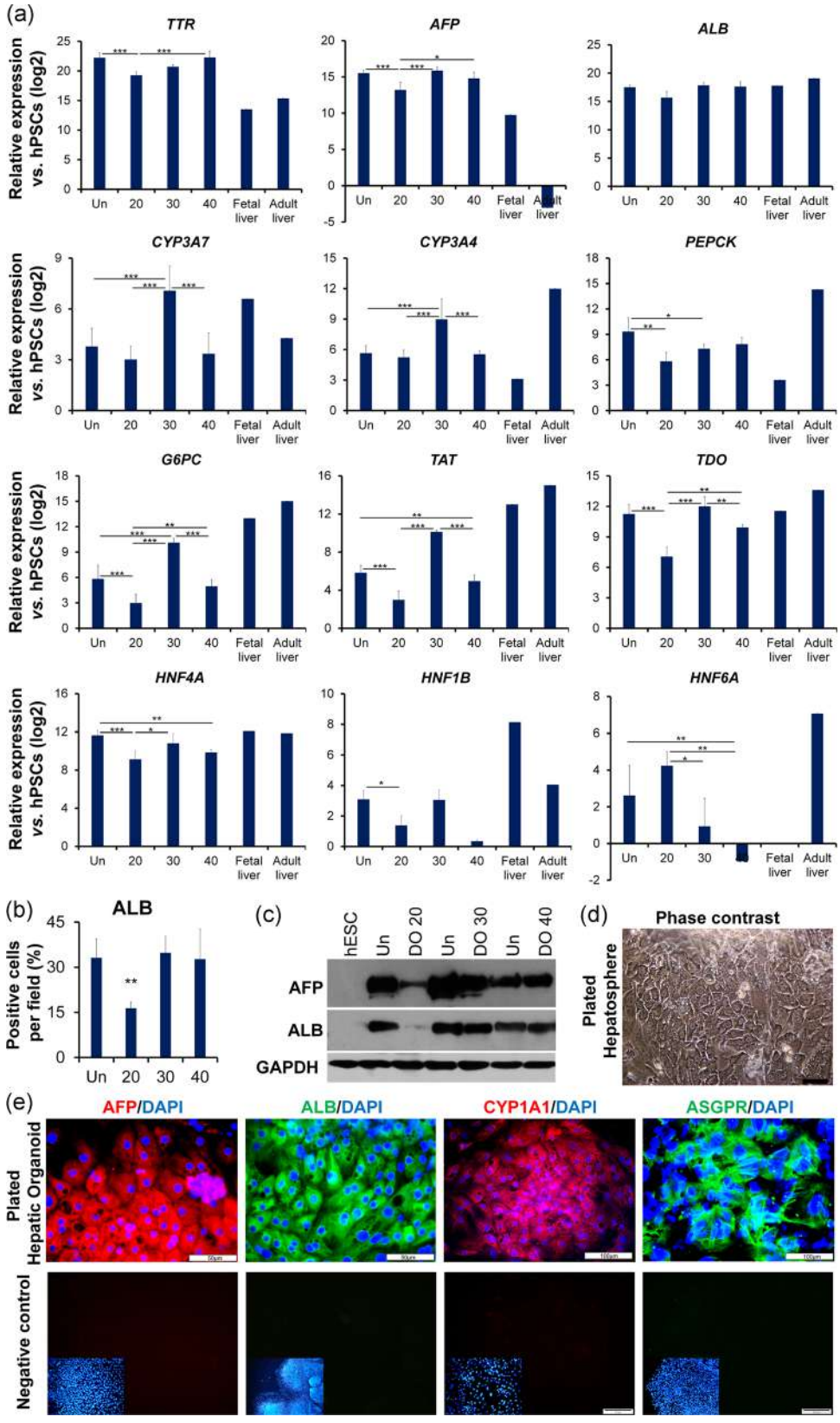
(a)
TTR
AFP
ALB
CYP3A7
CYP3A4
PEPCK
G6PC
TAT
TDO
HNF4A
HNF1B
HNF6A
Relative expression vs. hPSCs (log2)
Un
20
30
40
Fetal liver
Adult liver
(b)
ALB
Positive cells per field (%)
(c)
hESC
Un
DO 20
DO 30
DO 40
AFP
ALB
GAPDH
(d)
Phase contrast
Plated Hepatosphere
(e)
AFP/DAPI
ALB/DAPI
CYP1A1/DAPI
ASGPR/DAPI
Plated Hepatic Organoid
Negative control

runs under the 30% DO concentration. Similar gene expression profiles and culture outcomes confirmed the reproducibility of this established protocol (Figure 7a). We showed that increasing the integrated hepatic differentiation working volume from 50 to 150 ml without key bioprocess parameter controls (DO and pH) caused a significant decrease in mature hepatic differentiation, which could be overcome by conducting the process at 30% DO under fully controlled culture conditions in the stirred bioreactor (Figure 7b,c).

4 | DISCUSSION

Previously, we developed a scalable culture system for large-scale production of hepatocytes from hPSC aggregates under a dynamic suspension culture. However, that protocol suffered from low differentiation efficacy, decreased hepatosphere size, lack of a homogeneous morphology (approximately 50% cystic and 50% dense spheres, and poor productivity; Vosough et al., 2013). It has been reported that cystic or dense hepatospheres generated under uncontrolled culture conditions exhibited differences in hepatic markers expression levels and their spatial distribution within the hepatospheres. For instance, dense hepatospheres contained higher percentages of hepatocytes that expressed mature specific markers, whereas the same markers were downregulated in hepatocytes populated in cystic hepatospheres. Subsequently, we attempted to improve the efficacy of this protocol by establishing a cost-effective, efficient differentiation process to optimize the size of the initial hPSC aggregates before starting integrated hepatic differentiation under a dynamic suspension culture in a 50 ml working volume. Optimization trials resulted in improved efficacy of the differentiation protocol with decreased cystic hepatospheres formation with poor functionality and improved hepatocyte function inside the cystic hepatospheres (Farzaneh et al., 2018). Then, we attempted to scale up this protocol for large-scale production of functional hepatocyte-like cells from hPSCs. However, scale-up trials with only three-fold (150 ml) working volume with the same improved and optimized differentiation protocol were not successful since significant increase in cystic hepatosphere generation and decreased expressions of some important mature hepatic markers along with their significant downregulation observed during the integrated differentiation process. Therefore, we determined that the poor scalability of the uncontrolled culture condition was a critical issue that should be addressed before translating established protocols to clinical or commercial applications. Here, we monitored the key bioprocess parameters during integrated and stepwise hepatic differentiation in the bioreactor with 150 ml working volume under uncontrolled culture condition. It was our intent to explore possible limiting parameters that resulted in the generation of hepatospheres with low functionality. We observed that pH values and DO concentration were largely unstable and had a decreasing trend during integrated hepatic differentiation. Practically, the DO concentration profile suddenly decreased during the hepatoblast phase (Day 9 of culture) as determined by online monitoring of these parameters during 20 days of culture. We hypothesized that the DO concentration was a limiting and important factor during the hepatocyte expansion/maturation phase, which possibly affected the efficacy and productivity of the hepatic differentiation process. Theoretically, the amount of oxygen available for cells can become limited when expansion and integrated differentiation is conducted with large culture working volumes (i.e., more than 1 L) under dynamic suspension without DO and pH control because of a lower cell culture surface to volume ratio (e.g., spinner flask culture). Under uncontrolled cultures, the amount of DO largely depends on culture vessel geometry, agitation speed, liquid/air interface area to depth of the medium ratio, cell density, cellular respiration, and oxygen level in the incubator (Csete, 2005; Wion, Christen, Barbier, & Coles, 2009).

Several studies have demonstrated the critical effects of the oxygen concentration/gradient as a developmental morphogen and cell fate modulator (e.g., stem cell maintenance or cellular differentiation) in a concentration-dependent manner for neural, cardiomyocyte, endoderm, and mesodermal lineages, which were mainly under static culture conditions with limited working volumes (Horton & Auguste, 2012; Medley et al., 2013; Niebruegge et al., 2009).

Regarding hepatic differentiation of hPSCs, it has been shown that a hypoxic or normoxic culture condition can regulate the differentiation process efficacy and outcome. Hypoxic culture conditions can promote mesoderm, endoderm, and hepatoblast differentiation; however, it has an adverse effect on haptic endoderm cell proliferation and maturation, which will lead to inhibition of mature hepatocyte induction in a 2D adherent culture (van Wenum et al., 2018). The hypoxic culture condition activates hypoxia-inducible factors (HIF-1a molecules that control and regulate stem

FIGURE 5 The gene and protein expression of the hepatic organoids. (a) Gene expression analysis of hepatic organoids showed that hepatic gene expression in 20% DO was significantly lower than the uncontrolled condition. Expression of some mature genes in the 30% DO condition was significantly higher than under the uncontrolled condition. (b) The percentage of ALB-positive cells in the hepatic organoid cell population was calculated by counting positive cells from different immunofluorescent images of sectioned hepatospheres generated in 30% DO. (c) Western blot for AFP and ALB expression in hepatic organoids. (d) Representative phase contrast images of plated hepatic organoid. (e) Immunofluorescent staining of plated hepatic organoids AFP, ALB, CYP1A1, and ASGPR as mature hepatic markers in the 30% DO condition. Scale bar = 50 μm. Data (mean ± *SD*) were analyzed with ANOVA and Tukey's post hoc test; $n = 3$. 20%, 30%, and 40%, differentiation under DO controlled culture conditions; AFP, α-fetoprotein; ALB, albumin. ANOVA, analysis of variance; DAPI, 4′,6-diamidino-2-phenylindole; DO, dissolved oxygen; GAPDH, glyceraldehyde 3-phosphate dehydrogenase; Un, differentiation under uncontrolled culture condition. $^{*}p < .05$; $^{**}p < .01$; $^{***}p < .001$ [Color figure can be viewed at wileyonlinelibrary.com]

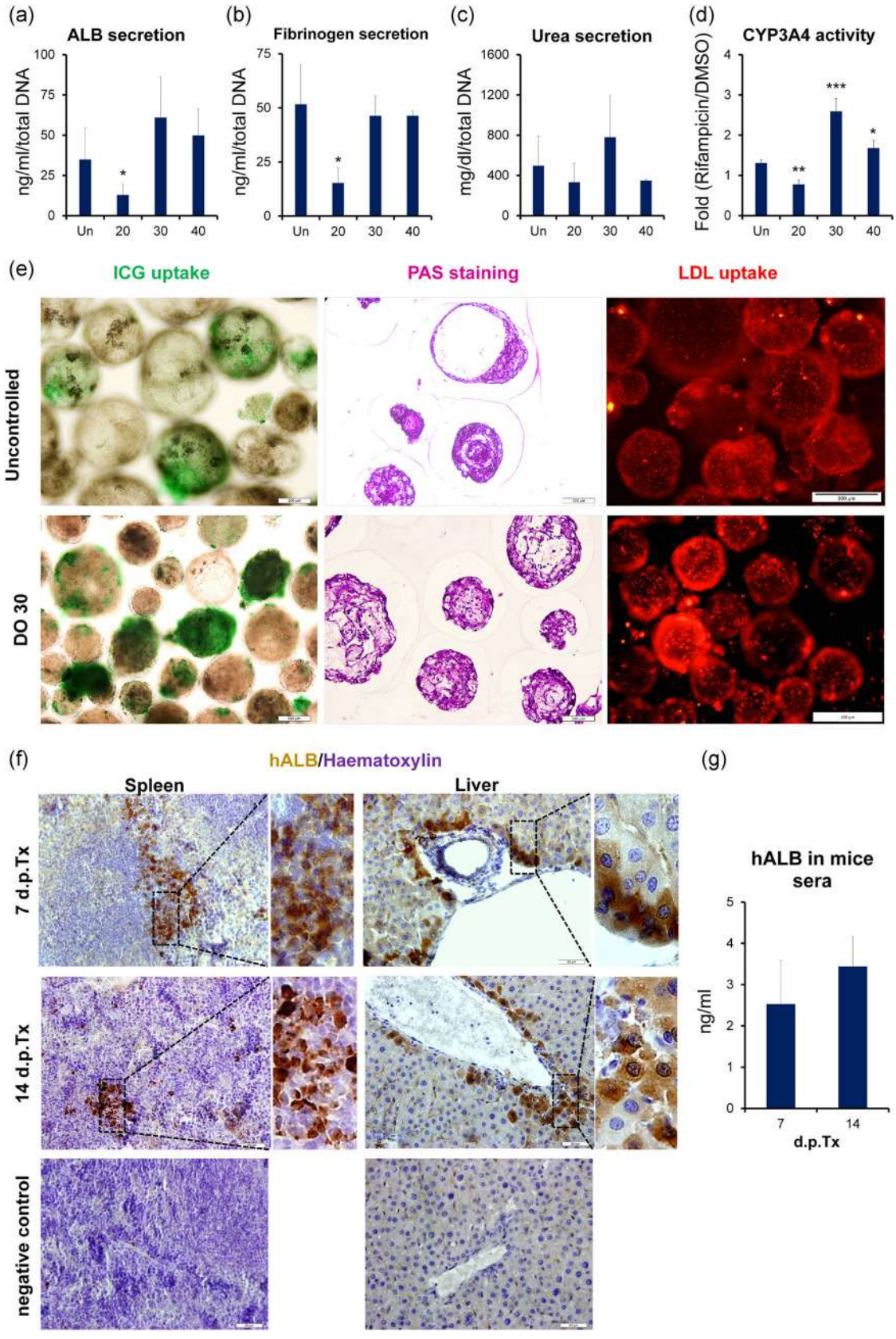
(a)
ALB secretion
ng/ml/total DNA
100
75
50
25
0
Un
20
30
40
(b)
Fibrinogen secretion
ng/ml/total DNA
75
50
25
0
(c)
Urea secretion
mg/dl/total DNA
1600
1200
800
400
0
(d)
CYP3A4 activity
Fold (Rifampicin/DMSO)
4
3
2
1
0
**
***
*
(e)
ICG uptake
PAS staining
LDL uptake
Uncontrolled
DO 30
(f)
hALB/Haematoxylin
Spleen
Liver
7 d.p.Tx
14 d.p.Tx
negative control
(g)
hALB in mice sera
ng/ml
5
4
3
2
1
0
7
14
d.p.Tx

cell behavior and regulate the Wnt, Notch, and TGFB signaling pathways; Bogaerts, Heindryckx, Vandewynckel, Van Grunsven, & Van Vlierberghe, 2014) that promote differentiation of hepatoblasts to a cholangiocyte fate (Ayabe et al., 2018). However, it has been shown to decrease the metabolism, functional polarization, gene expression, and drug clearance of hepatocytes (Kidambi et al., 2009). CYP3A4, a hepatic maturation marker, has been shown to down-regulate under hypoxic conditions and recover under normoxic culture conditions (van Wenum et al., 2018). Thus, a hypoxic culture condition (2%–5% O_2) is not efficient for the entire hepatic differentiation process. Proliferation of hepatic progenitors and their further maturation would require a normoxic culture condition (20% O_2).

The significant effect of DO concentration on the integrated differentiation process under dynamic suspension culture was reported for different cell types, including neural cells (Serra, Brito, Costa, Sousa, & Alves, 2009), red blood cells (Bayley et al., 2018), and skin-derived precursor cells (Agabalyan et al., 2017) that were produced in fully controlled bioreactors. However, for liver and integrated hepatic differentiation of hPSCs, most studies were conducted in small scale culture systems under uncontrolled culture conditions in an attempt to explore the role of the oxygen concentration/gradient in hepatic differentiation and functionality, liver development, and primary hepatocyte maintenance and function.

In terms of the effect of oxygen concentration on hepatocyte structure and metabolic activity in human liver tissue, an oxygen concentration gradient exists in the adult liver lobule that induces the formation of three different zones in the liver for over 500 total metabolic activities. Around the portal vein, the oxygen concentration is approximately 60–65 mmHg, whereas it decreases to 30–35 mmHg in regions closer to the central vein (Kietzmann, 2017). Gluconeogenesis and ureagenesis occur in the majority of periportal hepatocytes, whereas the pericentral zone is the site of glycolysis and detoxification activities (Kietzmann, 2017).

However, there is no report about the effect of physiological levels of DO concentrations during the integrated hepatic differentiation process and large-scale production of hPSC-derived hepatocytes in fully controlled bioreactors. Therefore, we evaluated three DO concentration levels (20%, 30%, and 40% equal to 30, 45, and 60 mmHg at 37°C, respectively) in the range of human liver tissue oxygen concentration levels (30–60 mmHg pO_2 at different regions) combined with an automatic pH control of 7.1 ± 0.1 to explore the effect of these DO concentrations on hepatic organoid formation.

Our data showed that high oxygen concentrations (30% and 40% DO) had no significant effects on endoderm and hepatic endoderm differentiation efficacy compared to the uncontrolled culture condition. The 20% DO concentration generated hepatic endoderm that had poor functionality. The uncontrolled culture condition with 150 ml working volume had a DO concentration range between 50%–70% after media refreshment during endoderm and hepatic endoderm generation; therefore, it could not be considered a limiting factor. Thus, the lower DO concentration (20%) that resulted in lower hepatic endoerm markers gene expression is not efficint and DO concentration above 30% should be employed during the integrated hepatic endoderm generation phase.

During the hepatic endoderm proliferation and maturation phase, the 30% DO concentration generated functional fetal-like liver organoids that had a uniform size and better homogeneity. Interestingly, different DO concentrations also resulted in hepatocytes that were generated with different metabolic activities and functionalities or mixed cell populations. For instance, there were significantly greater *G6PC* gene expression, which functions in the gluconeogenesis and glycogenolysis processes, and *CYP3A7* and *CYP3A4* activities (as xenobiotic factors responsible for the detoxification process) in the 30% DO, which resembled the oxygen concentration in the pericentral liver zone. It was reported that rat hepatocytes culture in a 30% DO controlled bioreactor resulted in long-term maintenance of metabolic activity compared to the uncontrolled culture condition (Miranda et al., 2009).

At 40% DO, there was no difference in the expression levels of the related genes compared to the uncontrolled condition, whereas more erythrocyte cells were produced compared to 30% DO due to induction of erythroid cell generation by the higher DO concentration. Thus, hepatocytes with special zone characteristics might be produced if we extended the differentiation process for a longer period and regulated the oxygen concentration at different levels.

Another important outcome of this study is the regulation effect of the oxygen concentration (30% and 40% DO) on hPSCs fate and generation of hepatic organoids that consisted of red blood cells and functional hepatocyte-like cells with similar characteristics to the human fetal liver cell population (Dzierzak & Speck, 2008). During embryogenesis, primary erythropoiesis transfers from the yolk sac to

FIGURE 6 The functional activity of hepatic organoids. The hepatic organoids performed major hepatic functions. (a) ALB and (b) fibrinogen secretion. ALB and fibrinogen secretions decreased significantly in the 20% DO. (c) Urea secretion. (d) Evaluation of the detoxification activity. Data showed that CYP3A4 enzyme activity increased significantly in response to rifampicin compared to DMSO as the control group under 30% DO and it reduced under 20% DO. (e) Representative images for uptake of LDL, stored glycogen in their cytoplasm, and ICG under the uncontrolled culture condition and 30% DO. Scale bar = 100 μm. (f) Engraftment of hepatic organoids cells derived under 30% DO in mice spleen. Representative immunohistochemistry images showed the transplanted hepatic organoid cells distributed as clusters or single human ALB-positive cells in the spleen and liver of mice at days 7 and 14 post-transplantation. (g) Engrafted cells secreted human ALB into mice sera at Days 7 and 14. Data are mean ± *SD* and analyzed with ANOVA and Tukey's post hoc test; $n = 3$; 20%, 30% and 40%, differentiation under DO controlled culture conditions; AFP, alpha-fetoprotein; ALB, albumin. ANOVA, analysis of variance; DO, dissolved oxygen; Un, differentiation under uncontrolled culture condition. $^{**}p < .01$; $^{***}p < .001$ [Color figure can be viewed at wileyonlinelibrary.com]

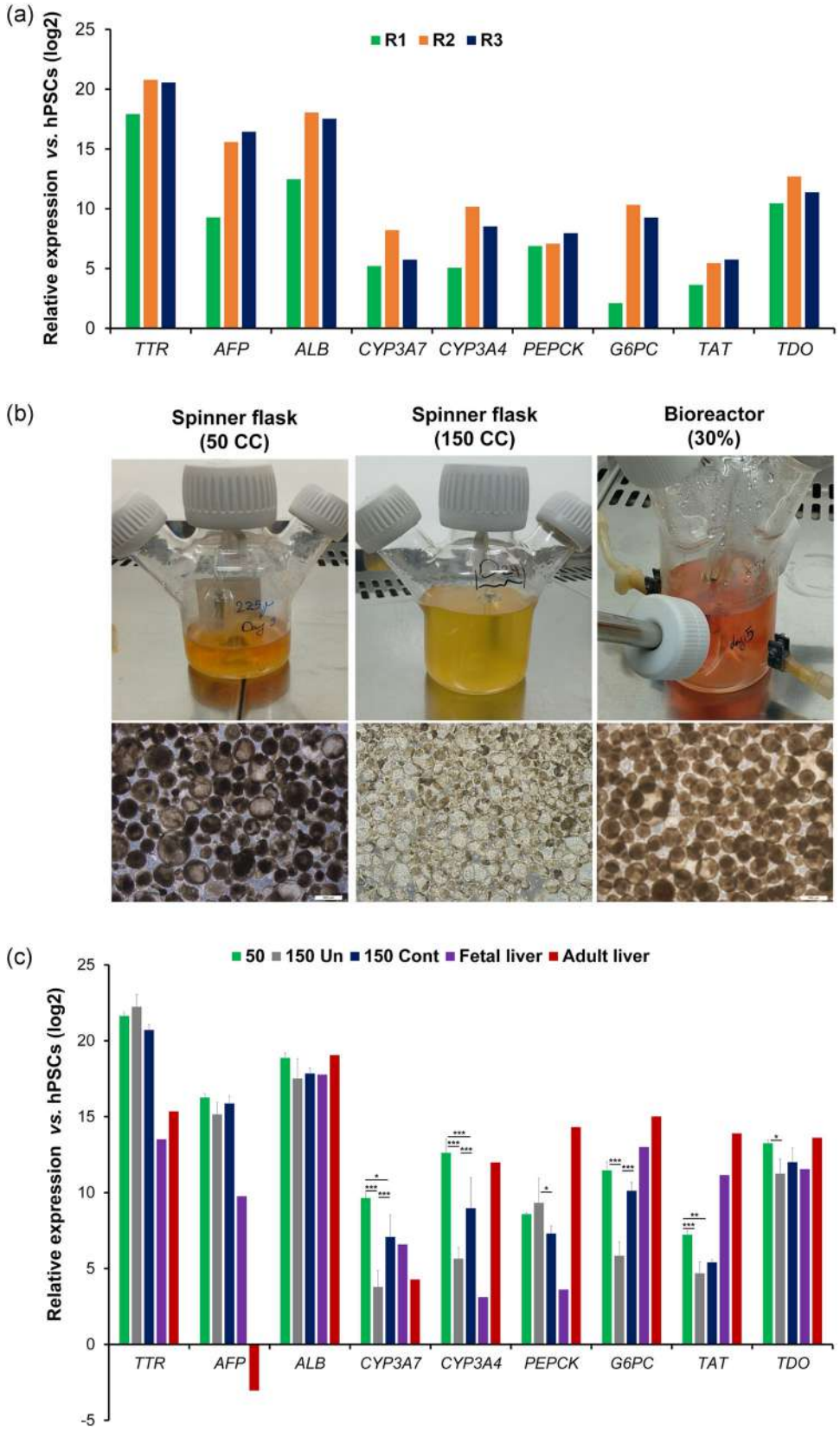

FIGURE 7 Validation of the developed integrated hepatic differentiation protocol at 30% DO concentration. (a) Important hepatic marker gene expressions in fetal-like hepatic organoids generated with three different bioreactor runs at 30% DO concentration. (b) Production of hepatic organoids under uncontrolled (50 and 150 ml) and fully controlled conditions (30% DO, 150 ml). (c) Their important hepatic marker gene expression compared to the fetal and adult livers. Data (mean ± *SD*) were analyzed with ANOVA and Tukey's post hoc test; $n = 3$. ANOVA, analysis of variance; DO, dissolved oxygen. $^{*}p < .01$; $^{**}p < .01$; $^{***}p < .001$ [Color figure can be viewed at wileyonlinelibrary.com]

the fetal liver and definitive erythropoiesis occurs (Palis, 2014). The resident hepatoblasts secrete erythropoietic cytokines such as stem cell factor (SCF) and erythropoietin to promote differentiation of hematopoietic stem cells to erythroid cells and produce red blood cells (Sugiyama, Kulkeaw, Mizuochi, Horio, & Okayama, 2011).

Although the production of red blood cells in conjunction with hepatocytes can result in decreased hepatocyte production, it resulted in improved functionality of the hepatocytes generated under 30% DO with higher CYP activities, which was possibly due to cell-cell interaction and cross-talk between these two cell populations. HSC secrete OSM, which promotes hepatocyte maturation (Kinoshita & Miyajima, 2002). We demonstrated that erythroblasts produced within our hepatic organoids under 30% and 40% DO conditions have a fetal identity similar to cells generated during fetal liver development.

Therefore, we hypothesized that this was a direct result of regulating oxygen concentrations over 30% DO and inducing co-generation of mesoderm and endoderm cells within the hPSCs aggregates from Day 3 of the integrated differentiation process. This was confirmed by qRT-PCR analysis of mesoderm related genes, which showed significant upregulation of *MIXL1* under 30% and 40% DO compared to the uncontrolled culture condition, as well as *T* to a lesser extent on Day 3 of differentiation. Previous studies showed that a hypoxic culture condition (Ramírez-Bergeron et al., 2004) and treatment with CHIR99021 (Galat et al., 2018) could promote mesoderm and hemangioblast differentiation of hPSCs. We had 1 day of CHIR treatment in our protocol that mainly induced mesoendoderm generation and activin treatment that mainly promoted endoderm differentiation (Farzaneh et al., 2018). We believe that the higher DO concentration regulated the CHIR treated/mesoendoderm induced hPSC aggregate fate and induced mesoderm differentiation in parallel with endoderm differentiation. Ji et al. (2010) reported similar results and concluded that reactive oxygen species enhanced differentiation of human embryonic stem cells into a mesendodermal lineage under a static culture condition.

The fully controlled culture at 30% and 40% DO resulted in enhanced expressions of some hematopoietic progenitor cell-related genes (*RUNX1*, *HOXA9*, *HOXB4*, *DLL4*, and *PECAM*) compared to the uncontrolled culture condition on Day 9 of culture. However, most of these hematopoietic specific markers and receptors are common with hepatic progenitor cells and could not be solely related to erythropoietic differentiation. This similarity made HSC generation tracking difficult during the integrated hepatic differentiation. It has been reported that hepatic progenitor cells derived from hPSCs also expressed CD31, CD133, and GATA2 markers that are also related to hematopoietic cell markers (Goldman et al., 2016). Nevertheless, the expression of erythroid related genes was higher under controlled conditions from the hepatic endoderm generation step to further maturation and generation of functional hepatic organoids.

Finally, we injected whole organoids into the spleens of mice that had induced acute liver injuries to assess the transplantability of these fetal liver organoids that were generated under the fully controlled 30% DO condition. The results showed the existence of viable and metabolically active human ALB-positive cells and clusters in the spleens of this animal model 7- and 14-day post-transplantation, along with their increased metabolic activity as demonstrated by increased levels of human ALB in mice sera 2 weeks after the transplantation.

5 | CONCLUSION

We have developed a scalable platform for fully controlled large-scale production of hepatic organoids by optimizing DO concentration during the integrated differentiation process. Our data emphasize that oxygen concentration is a very important bioprocess parameter that regulates proliferation, differentiation efficacy, and generated hepatocyte metabolic activity. Thus, this parameter should be carfully optimized during the integrated hepatic differentiation process for a scalable production of hepatic cells. The results show that the oxygen concentration regulates the fate of these hPSC aggregates by inducing simultaneous endoderm and mesoderm in a concentration-dependent manner, which results in the generation of fetal-like hepatic organoids and red blood cells. The functionality and metabolic activities of hepatocytes were improved at 30% DO. The oxygen switching during differentiation could be used to generate hepatocytes with different metabolic activity profiles that mimic those different zones of liver tissue. This integrated hepatic differentiation strategy might facilitate large-scale production of organoids for potential medical applications, fabrication of liver tissues/organs in the laboratory, and drug discovery applications.

ACKNOWLEDGMENTS

We express our appreciation to Hassan Ansari at Royan Institute for his technical assistance. This study was funded by Royan Institute, the Iranian Council of Stem Cell Research and Technology, the Iran National Science Foundation (INSF), and the Ministry of Health and Medical Education (No. 56700/147) to H. B.

CONFLICT OF INTERESTS

The authors declare that there are no conflict of interests.

ORCID

Zahra Farzaneh http://orcid.org/0000-0001-5234-9026
Mehdi Alikhani http://orcid.org/0000-0002-8808-9577
Joaquim M. S. Cabral http://orcid.org/0000-0002-2405-5845
Hossein Baharvand http://orcid.org/0000-0001-6528-3687

REFERENCES

Abbasalizadeh, S., Larijani, M. R., Samadian, A., & Baharvand, H. (2012). Bioprocess development for mass production of size-controlled human pluripotent stem cell aggregates in stirred suspension bioreactor. *Tissue Engineering. Part C, Methods*, *18*(11), 831–851. https://doi.org/10.1089/ten.TEC.2012.0161

Agabalyan, N. A., Borys, B. S., Sparks, H. D., Boon, K., Raharjo, E. W., Abbasi, S., … Biernaskie, J. (2017). Enhanced expansion and sustained inductive function of skin-derived precursor cells in

computer-controlled stirred suspension bioreactors. *Stem Cells Translational Medicine*, *6*(2), 434–443. https://doi.org/10.5966/sctm.2016-0133

Alwahsh, S. M., Rashidi, H., & Hay, D. C. (2018). Liver cell therapy: Is this the end of the beginning? *Cellular and Molecular Life Science*, *75*(8), 1307–1324. https://doi.org/10.1007/s00018-017-2713-8

Ayabe, H., Anada, T., Kamoya, T., Sato, T., Kimura, M., Yoshizawa, E., … Taniguchi, H. (2018). Optimal hypoxia regulates human iPSC-derived liver bud differentiation through intercellular TGFB signaling. *Stem Cell Reports*, *11*(2), 306–316. https://doi.org/10.1016/j.stemcr.2018.06.015

Ayllon, V., Bueno, C., Ramos-Mejia, V., Navarro-Montero, O., Prieto, C., Real, P. J., … Menendez, P. (2015). The Notch ligand DLL4 specifically marks human hematoendothelial progenitors and regulates their hematopoietic fate. *Leukemia*, *29*(8), 1741–1753. https://doi.org/10.1038/leu.2015.74

Baumann, C. I., Bailey, A. S., Li, W., Ferkowicz, M. J., Yoder, M. C., & Fleming, W. H. (2004). PECAM-1 is expressed on hematopoietic stem cells throughout ontogeny and identifies a population of erythroid progenitors. *Blood*, *104*(4), 1010–1016. https://doi.org/10.1182/blood-2004-03-0989

Bayley, R., Ahmed, F., Glen, K., McCall, M., Stacey, A., & Thomas, R. (2018). The productivity limit of manufacturing blood cell therapy in scalable stirred bioreactors. *Journal of Tissue Engineering and Regenerative Medicine*, *12*(1), e368–e378. https://doi.org/10.1002/term.2337

Bogaerts, E., Heindryckx, F., Vandewynckel, Y. P., Van Grunsven, L. A., & Van Vlierberghe, H. (2014). The roles of transforming growth factor-beta, Wnt, Notch and hypoxia on liver progenitor cells in primary liver tumours (Review). *International Journal of Oncology*, *44*(4), 1015–1022. https://doi.org/10.3892/ijo.2014.2286

Brandt, S. J., & Koury, M. J. (2009). Regulation of LMO2 mRNA and protein expression in erythroid differentiation. *Haematologica*, *94*(4), 447–448. https://doi.org/10.3324/haematol.2008.005140

Brooks, A. J., Hammond, J. S., Girling, K., & Beckingham, I. J. (2007). The effect of hepatic vascular inflow occlusion on liver tissue pH, carbon dioxide, and oxygen partial pressures: Defining the optimal clamp/release regime for intermittent portal clamping. *Journal of Surgical Research*, *141*(2), 247–251. https://doi.org/10.1016/j.jss.2006.10.054

Burda, P., Laslo, P., & Stopka, T. (2010). The role of PU.1 and GATA-1 transcription factors during normal and leukemogenic hematopoiesis. *Leukemia*, *24*(7), 1249–1257. https://doi.org/10.1038/leu.2010.104

Csete, M. (2005). Oxygen in the cultivation of stem cells. *Annals of the New York Academy of Sciences*, *1049*, 1–8. https://doi.org/10.1196/annals.1334.001

Dutkowski, P., Linecker, M., DeOliveira, M. L., Mullhaupt, B., & Clavien, P. A. (2015). Challenges to liver transplantation and strategies to improve outcomes. *Gastroenterology*, *148*(2), 307–323. https://doi.org/10.1053/j.gastro.2014.08.045

Dzierzak, E., & Speck, N. A. (2008). Of lineage and legacy: The development of mammalian hematopoietic stem cells. *Nature Immunology*, *9*(2), 129–136. https://doi.org/10.1038/ni1560

Farzaneh, Z., Najarasl, M., Abbasalizadeh, S., Vosough, M., & Baharvand, H. (2018). Developing a cost-effective and scalable production of human hepatic competent endoderm from size-controlled pluripotent stem cell aggregates. *Stem Cells and Development*, *27*(4), 262–274. https://doi.org/10.1089/scd.2017.0074

Fonoudi, H., Ansari, H., Abbasalizadeh, S., Larijani, M. R., Kiani, S., Hashemizadeh, S., … Baharvand, H. (2015). A universal and robust integrated platform for the scalable production of human cardiomyocytes from pluripotent stem cells. *Stem Cells Translational Medicine*, *4*(12), 1482–1494. https://doi.org/10.5966/sctm.2014-0275

Forrester, L. M., & Jackson, M. (2012). Mechanism of action of HOXB4 on the hematopoietic differentiation of embryonic stem cells. *Stem Cells*, *30*(3), 379–385. https://doi.org/10.1002/stem.1036

Galat, Y., Elcheva, I., Dambaeva, S., Katukurundage, D., Beaman, K., Iannaccone, P. M., & Galat, V. (2018). Application of small molecule CHIR99021 leads to the loss of hemangioblast progenitor and increased hematopoiesis of human pluripotent stem cells. *Experimental Hematology*, *65*, 38–48. https://doi.org/10.1016/j.exphem.2018.05.007

Goldman, O., Cohen, I., & Gouon-Evans, V. (2016). Functional blood progenitor markers in developing human liver progenitors. *Stem Cell Reports*, *7*(2), 158–166. https://doi.org/10.1016/j.stemcr.2016.07.008

Han, S., Goldman, O., & Gouon-Evans, V. (2014). Liver progenitor cell and KDR. *Cell Cycle*, *13*(7), 1051–1052. https://doi.org/10.4161/cc.28213

Horton, R. E., & Auguste, D. T. (2012). Synergistic effects of hypoxia and extracellular matrix cues in cardiomyogenesis. *Biomaterials*, *33*(27), 6313–6319. https://doi.org/10.1016/j.biomaterials.2012.05.063

Ji, A.-R., Ku, S.-Y., Cho, M. S., Kim, Y. Y., Kim, Y. J., Oh, S. K., … Choi, Y. M. (2010). Reactive oxygen species enhance differentiation of human embryonic stem cells into mesendodermal lineage. *Experimental & Molecular Medicine*, *42*(3), 175–186.

Jungermann, K., & Kietzmann, T. (2000). Oxygen: Modulator of metabolic zonation and disease of the liver. *Hepatology*, *31*(2), 255–260. https://doi.org/10.1002/hep.510310201

Khakpour, S., Di Renzo, A., Curcio, E., Di Maio, F. P., Giorno, L., & De Bartolo, L. (2017). Oxygen transport in hollow fibre membrane bioreactors for hepatic 3D cell culture: A parametric study. *Journal of Membrane Science*, *544*, 312–322.

Kidambi, S., Yarmush, R. S., Novik, E., Chao, P., Yarmush, M. L., & Nahmias, Y. (2009). Oxygen-mediated enhancement of primary hepatocyte metabolism, functional polarization, gene expression, and drug clearance. *Proceedings of the National Academy of Sciences of the United States of America*, *106*(37), 15714–15719. https://doi.org/10.1073/pnas.0906820106

Kietzmann, T. (2017). Metabolic zonation of the liver: The oxygen gradient revisited. *Redox Biology*, *11*, 622–630. https://doi.org/10.1016/j.redox.2017.01.012

Kinoshita, T., & Miyajima, A. (2002). Cytokine regulation of liver development. *Biochimica et Biophysica Acta/General Subjects*, *1592*(3), 303–312. https://doi.org/10.1016/s0167-4889(02)00323-3

Kwok, C. K., Ueda, Y., Kadari, A., Gunther, K., Ergun, S., Heron, A., … Edenhofer, F. (2018). Scalable stirred suspension culture for the generation of billions of human induced pluripotent stem cells using single-use bioreactors. *Journal of Tissue Engineering and Regenerative Medicine*, *12*(2), e1076–e1087. https://doi.org/10.1002/term.2435

Laurenti, E., Doulatov, S., Zandi, S., Plumb, I., Chen, J., April, C., … Dick, J. E. (2013). The transcriptional architecture of early human hematopoiesis identifies multilevel control of lymphoid commitment. *Nature Immunology*, *14*(7), 756–763. https://doi.org/10.1038/ni.2615

Medley, T. L., Furtado, M., Lam, N. T., Idrizi, R., Williams, D., Verma, P. J., … Kaye, D. M. (2013). Effect of oxygen on cardiac differentiation in mouse iPS cells: Role of hypoxia inducible factor-1 and Wnt/beta-catenin signaling. *PLOS One*, *8*(11), e80280. https://doi.org/10.1371/journal.pone.0080280

Miranda, J. P., Leite, S. B., Muller-Vieira, U., Rodrigues, A., Carrondo, M. J., & Alves, P. M. (2009). Towards an extended functional hepatocyte in vitro culture. *Tissue Engineering. Part C, Methods*, *15*(2), 157–167. https://doi.org/10.1089/ten.tec.2008.0352

Nemati, S., Abbasalizadeh, S., & Baharvand, H. (2016). Scalable expansion of human pluripotent stem cell-derived neural progenitors in stirred suspension bioreactor under xeno-free condition. *Methods in Molecular Biology*, *1502*, 143–158. https://doi.org/10.1007/7651_2015_318

Ng, E. S., Azzola, L., Sourris, K., Robb, L., Stanley, E. G., & Elefanty, A. G. (2005). The primitive streak gene Mixl1 is required for efficient haematopoiesis and BMP4-induced ventral mesoderm patterning in differentiating ES cells. *Development*, *132*(5), 873–884. https://doi.org/10.1242/dev.01657

Niebruegge, S., Bauwens, C. L., Peerani, R., Thavandiran, N., Masse, S., Sevaptisidis, E., … Zandstra, P. W. (2009). Generation of human

embryonic stem cell-derived mesoderm and cardiac cells using size-specified aggregates in an oxygen-controlled bioreactor. *Biotechnology and Bioengineering*, *102*(2), 493–507. https://doi.org/10.1002/bit.22065

Nishikawa, M., Uchino, J., Matsushita, M., Takahashi, M., Taguchi, K., Koike, M., … Kon, H. (1996). Optimal oxygen tension conditions for functioning cultured hepatocytes in vitro. *Artificial Organs*, *20*(2), 169–177. https://doi.org/10.1111/j.1525-1594.1996.tb00723.x

Olson, J. C. (2016). Acute-on-chronic and decompensated chronic liver failure: Definitions, epidemiology, and prognostication. *Critical Care Clinics*, *32*(3), 301–309. https://doi.org/10.1016/j.ccc.2016.02.001

Palis, J. (2014). Primitive and definitive erythropoiesis in mammals. *Frontiers in Physiology*, *5*, 3. https://doi.org/10.3389/fphys.2014.00003

Pettinato, G., Lehoux, S., Ramanathan, R., Salem, M. M., He, L. X., Muse, O., … Fisher, R. A. (2019). Generation of fully functional hepatocyte-like organoids from human induced pluripotent stem cells mixed with endothelial cells. *Scientific Reports*, *9*(1), 8920. https://doi.org/10.1038/s41598-019-45514-3

Pimton, P., Lecht, S., Stabler, C. T., Johannes, G., Schulman, E. S., & Lelkes, P. I. (2015). Hypoxia enhances differentiation of mouse embryonic stem cells into definitive endoderm and distal lung cells. *Stem Cells and Development*, *24*(5), 663–676. https://doi.org/10.1089/scd.2014.0343

Ramírez-Bergeron, D. L., Runge, A., Dahl, K. D. C., Fehling, H. J., Keller, G., & Simon, M. C. (2004). Hypoxia affects mesoderm and enhances hemangioblast specification during early development. *Development*, *131*(18), 4623–4634.

Ramos-Mejia, V., Navarro-Montero, O., Ayllon, V., Bueno, C., Romero, T., Real, P. J., & Menendez, P. (2014). HOXA9 promotes hematopoietic commitment of human embryonic stem cells. *Blood*, *124*(20), 3065–3075. https://doi.org/10.1182/blood-2014-03-558825

Serra, M., Brito, C., Costa, E. M., Sousa, M. F., & Alves, P. M. (2009). Integrating human stem cell expansion and neuronal differentiation in bioreactors. *BMC Biotechnology*, *9*, 82. https://doi.org/10.1186/1472-6750-9-82

Sgodda, M., Dai, Z., Zweigerdt, R., Sharma, A. D., Ott, M., & Cantz, T. (2017). A scalable approach for the generation of human pluripotent stem cell-derived hepatic organoids with sensitive hepatotoxicity features. *Stem Cells and Development*, *26*(20), 1490–1504. https://doi.org/10.1089/scd.2017.0023

Shukla, A., Vadeyar, H., Rela, M., & Shah, S. (2013). Liver transplantation: East versus West. *Journal of Clinical and Experimental Hepatology*, *3*(3), 243–253. https://doi.org/10.1016/j.jceh.2013.08.004

Sugiyama, D., Kulkeaw, K., Mizuochi, C., Horio, Y., & Okayama, S. (2011). Hepatoblasts comprise a niche for fetal liver erythropoiesis through cytokine production. *Biochemical and Biophysical Research Communications*, *410*(2), 301–306. https://doi.org/10.1016/j.bbrc.2011.05.137

Takebe, T., Sekine, K., Enomura, M., Koike, H., Kimura, M., Ogaeri, T., … Taniguchi, H. (2013). Vascularized and functional human liver from an iPSC-derived organ bud transplant. *Nature*, *499*(7459), 481–484. https://doi.org/10.1038/nature12271

Takebe, T., Sekine, K., Kimura, M., Yoshizawa, E., Ayano, S., Koido, M., … Taniguchi, H. (2017). Massive and reproducible production of liver buds entirely from human pluripotent stem cells. *Cell Reports*, *21*(10), 2661–2670. https://doi.org/10.1016/j.celrep.2017.11.005

Tzanakakis, E. S., Hess, D. J., Sielaff, T. D., & Hu, W. S. (2000). Extracorporeal tissue engineered liver-assist devices. *Annual Review of Biomedical Engineering*, *2*, 607–632. https://doi.org/10.1146/annurev.bioeng.2.1.607

vanWenum, M., Adam, A. A. A., van der Mark, V. A., Chang, J. C., Wildenberg, M. E., Hendriks, E. J., … Hoekstra, R. (2018). Oxygen drives hepatocyte differentiation and phenotype stability in liver cell lines. *Journal of Cell Communication and Signaling*, *12*(3), 575–588. https://doi.org/10.1007/s12079-018-0456-4

Vicente, C., Conchillo, A., Garcia-Sanchez, M. A., & Odero, M. D. (2012). The role of the GATA2 transcription factor in normal and malignant hematopoiesis. *Critical Reviews in Oncology/Hematology*, *82*(1), 1–17. https://doi.org/10.1016/j.critrevonc.2011.04.007

Vosough, M., Omidinia, E., Kadivar, M., Shokrgozar, M. A., Pournasr, B., Aghdami, N., & Baharvand, H. (2013). Generation of functional hepatocyte-like cells from human pluripotent stem cells in a scalable suspension culture. *Stem Cells and Development*, *22*(20), 2693–2705. https://doi.org/10.1089/scd.2013.0088

Wion, D., Christen, T., Barbier, E. L., & Coles, J. A. (2009). PO(2) matters in stem cell culture. *Cell Stem Cell*, *5*(3), 242–243. https://doi.org/10.1016/j.stem.2009.08.009

Yamamoto, J., Udono, M., Miura, S., Sekiya, S., & Suzuki, A. (2018). Cell aggregation culture induces functional differentiation of induced hepatocyte-like cells through activation of hippo signaling. *Cell Reports*, *25*(1), 183–198. https://doi.org/10.1016/j.celrep.2018.09.010

Yzaguirre, A. D., deBruijn, M. F., & Speck, N. A. (2017). The role of Runx1 in embryonic blood cell formation. *Advances in Experimental Medicine and Biology*, *962*, 47–64. https://doi.org/10.1007/978-981-10-3233-2_4

Zhang, J., Zhao, X., Liang, L., Li, J., Demirci, U., & Wang, S. (2018). A decade of progress in liver regenerative medicine. *Biomaterials*, *157*, 161–176. https://doi.org/10.1016/j.biomaterials.2017.11.027

Ziegler, B. L., Valtieri, M., Porada, G. A., De Maria, R., Muller, R., Masella, B., … Peschle, C. (1999). KDR receptor: A key marker defining hematopoietic stem cells. *Science*, *285*(5433), 1553–1558. https://doi.org/10.1126/science.285.5433.1553

SUPPORTING INFORMATION

Additional supporting information may be found online in the Supporting Information section.

How to cite this article: Farzaneh Z, Abbasalizadeh S, Asghari-Vostikolaee M-H, Alikhani M, Cabral JMS, Baharvand H. Dissolved oxygen concentration regulates human hepatic organoid formation from pluripotent stem cells in a fully controlled bioreactor. *Biotechnology and Bioengineering*. 2020;1–18. https://doi.org/10.1002/bit.27521